

# EA303 WIND TUNNEL

## EXPERIMENT IV

### EFFECT OF ASPECT RATIO ON A FINITE WING

#### I. Purpose

1. Learn to operate the wind tunnel balance
  - a. measure lift, drag and pitching moment;
  - b. determine tare values;
  - c. correct data for model support effects.
2. Learn to reduce measured forces and moments to non-dimensionalized coefficient form.
3. Determine the effect of aspect ratio on lift, drag and pitching moment coefficients.
4. Experimentally determine the location of the aerodynamic center.
5. Measure the effect of angle-of-attack on wing lift and drag and wing pitching moment about the balance center. Determine the effect on wing pitching moment about the aerodynamic center.
6. Determine finite wing effects on lift, drag and pitching moment coefficient by comparing the measured results with NACA section data.
7. Observe Reynolds number effects by comparison with NACA data.

#### II. References

1. Abbott, I.H. and Von Doenhoff, A.E., *Theory of Wing Sections*, Dover Publications, Inc., 1959, Sec. 1.3.
2. Hurt, *Aerodynamics for Naval Aviators*, pp. 71–74.
3. Rae, W.H., Jr., and Pope, A., *Low Speed Wind Tunnel Testing*, John Wiley & Sons, New York, 1984, Sec. 4.1–4.16, 5.5.

#### III. Introduction

The purpose of most wind-tunnel experiments is to determine the aerodynamic forces and moments which act on a model and correct them for tunnel boundary, scale and Mach number effects. The simplest method to achieve this is to use a balance mechanism to measure forces and moments directly.

#### IV. Theory

The behavior of finite wings is an important concern in aircraft design. The variables of sweepback, section variation, geometric twist, taper, aspect ratio, tip shape and high-lift devices offer a wide spectrum of performance characteristics.

Variation of performance characteristics with aspect ratio,  $\mathcal{AR}$ , is of particular concern to a designer. Induced drag is inversely proportional to  $\mathcal{AR}$ , so it follows that a high aspect ratio wing is desirable for low speed/high lift coefficient operation. Although drag is then minimized, structural and weight problems arise due to long, thin planform configurations. High speed configurations at low lift coefficients and with sweepback for reduced wave drag usually lead to development of low aspect ratio wings. These, however, have poor low speed lifting and stability characteristics. A complete study of this variation gives the designer the tools to determine performance capabilities within design structural limitations.

Dimensional analysis indicates that

$$C_L, C_D, C_M = f(\alpha, \mathcal{AR}, \text{Re}, M)$$

where  $\mathcal{AR}$  is the aspect ratio. At low subsonic speeds, compressibility effects are negligible. Therefore

$$C_L, C_D, C_M = f(\alpha, \mathcal{AR}, \text{Re})$$

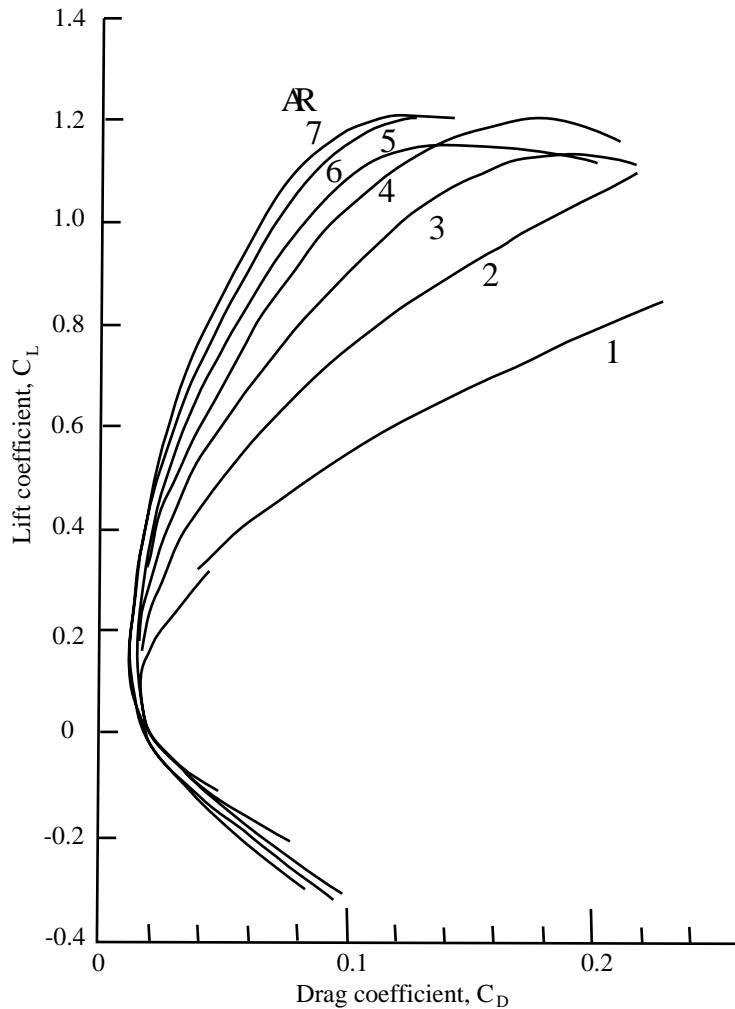


**Figure 4–1.** The effect of aspect ratio on the drag coefficient.

For a given test velocity the Reynolds number is a constant, thus

$$C_L, C_D, C_M = f(\alpha, \text{AR})$$

The effect of aspect ratio on the lift and drag of finite wings is shown in Figs. 4-1 and 4-2

For a given model, aspect ratio is fixed. Consequently

$$C_L, C_D, C_M = f(\alpha)$$

Comparison of  $C_L$ ,  $C_D$  and  $C_M$  vs  $\alpha$  curves for a finite wing with similar two-dimensional NACA airfoil results reveals the effects of aspect ratio. Comparison of slopes, intercepts, maxima, minima and general shape are valuable in defining these effects.

In general the aerodynamicist is most interested in  $dC_L/d\alpha$ ,  $C_{L\max}$ ,  $\alpha_{0L}$ ,  $C_{D0\min}$ , Oswald efficiency factor  $e$ , the aerodynamic center and  $C_{M_{ac}}$ .

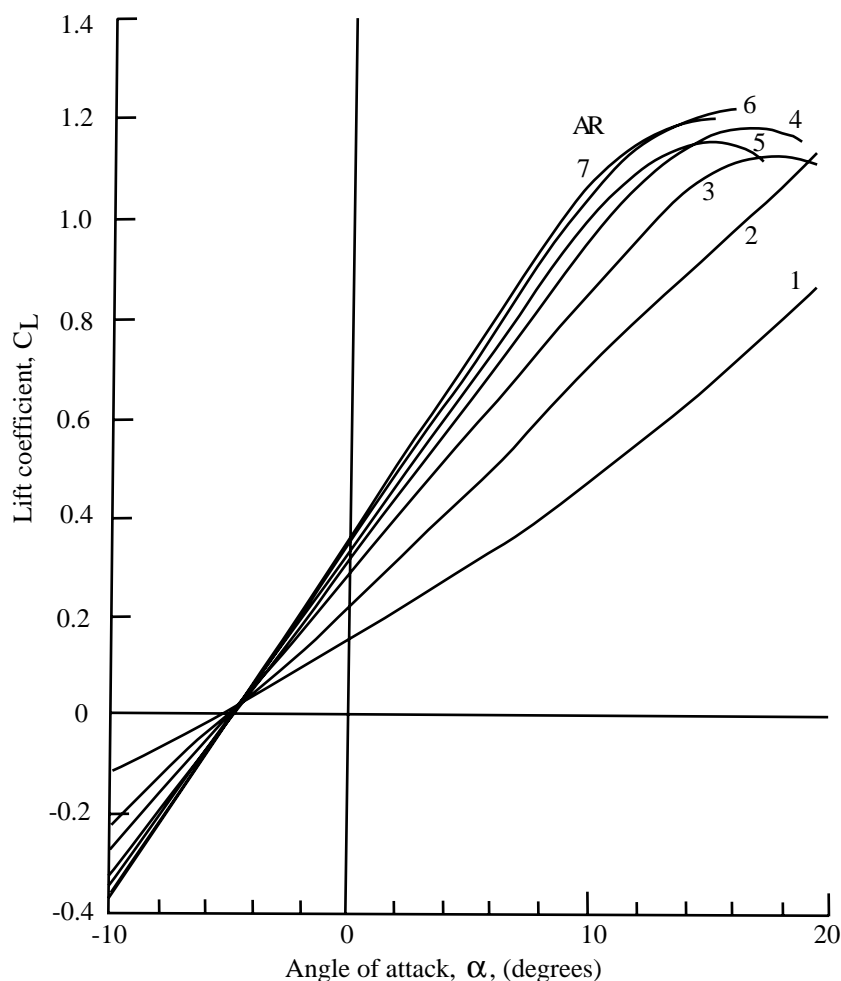


**Figure 4-2.** The effect of aspect ratio on the lift coefficient.

**The lift curve slope:  $dC_L/d\alpha$** 

Several theoretical analyses are available for predicting  $dC_L/d\alpha$ . Finite wing theory shows that the three-dimensional lift curve slope is given by

$$a = \frac{dC_L}{d\alpha} = \frac{a_0}{1 + \frac{a_0}{\pi \mathcal{AR}e_0}} \quad (1)$$

where  $a_0$  is the two-dimensional lift curve slope.

**Maximum lift coefficient:  $C_{L\max}$** 

Airfoil maximum lift coefficients vary from 0.6 to about 1.7. Finite wing maximum lift coefficients are from 85 to 90 percent of these values, and are never larger. It is a little known but well substantiated fact the  $C_{L\max}$  is affected by Mach number even in the low-speed range around  $M = 0.2$ . Thus, tests for maximum lift must be at the same landing Mach number as the proposed airplane.

**Angle of zero lift:  $\alpha_{0LW}$** 

The angle of zero lift in degrees is roughly equal to the amount of camber in percent of the airfoil chord.

**Minimum drag coefficient:  $C_{D_{0\min}}$** 

The minimum drag coefficient for airfoils decreases with increasing Reynolds number and generally has a value between 0.0050 and 0.0085.

**Spanwise efficiency factor:  $e$** 

The definition of the drag coefficient

$$C_D = C_{D_{0\min}} + \frac{C_L^2}{\pi \mathcal{AR}e} \quad (2)$$

makes the determination of spanwise efficiency factor,  $e$ , of importance. A plot of  $C_D$  versus  $C_L^2$  appears as a straight line with slight curvature at lower and higher values of  $C_L$ . The divergence at the low lift coefficients is a result of  $C_{D_{0\min}}$  not occurring at  $C_L = 0$  for a cambered airfoil. The divergence at higher  $C_L$ s is due to flow separation. The equation of the straight line is

$$C_D = C_{D_{0\min}} + KC_L^2 \quad (3)$$

and hence

$$K = \frac{1}{\pi \mathcal{AR}e} \quad (4)$$

and

$$e = \frac{1}{K\pi \mathcal{AR}} \quad (5)$$

The value of the spanwise efficiency factor,  $e$ , as defined above is about 0.85 to 0.95 for straight wings. An example is shown in Fig. 4-3.

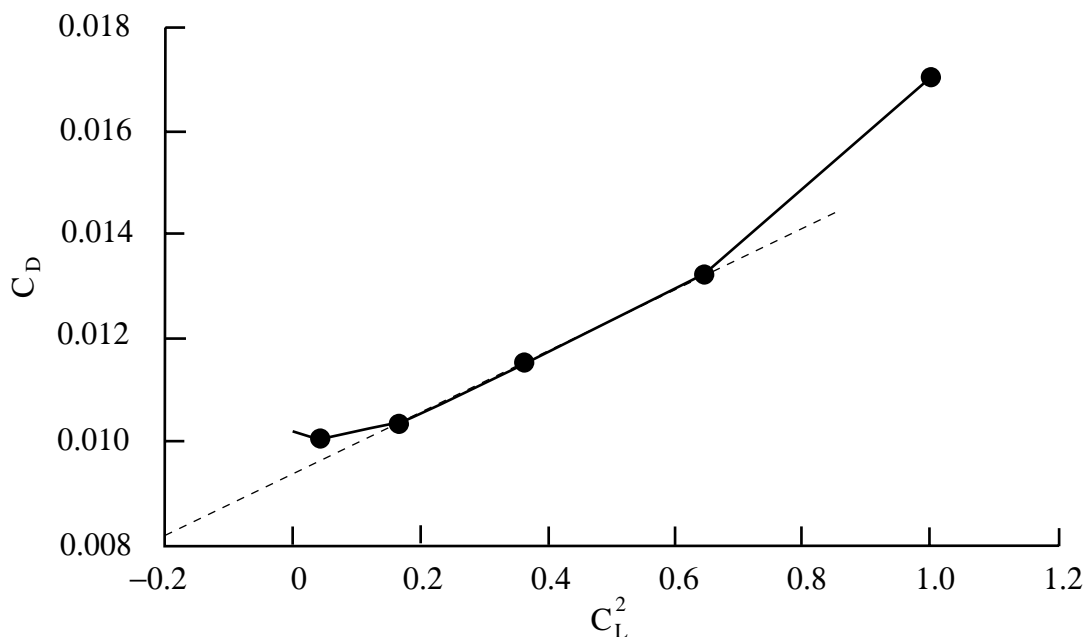


**Figure 4-3.**  $C_D$  versus  $C_L^2$  for an NACA 23012 wing

### Aerodynamic center

The location of the aerodynamic center is determined as follows:

Consider a wing mounted so that the axis of rotation is at some point behind and below the probable location of the aerodynamic center (Fig. 4-4).

Recall that the aerodynamic center is defined as the point about which the moment coefficient is not a function of angle of attack. Let the distance along the chord from the trunnion to the aerodynamic center be  $x_{ac}$ , and let the distance above the trunnion be  $y_{ac}$ .

The mean aerodynamic chord may be found from either

$$MAC = \frac{c_r + c_t}{2}$$

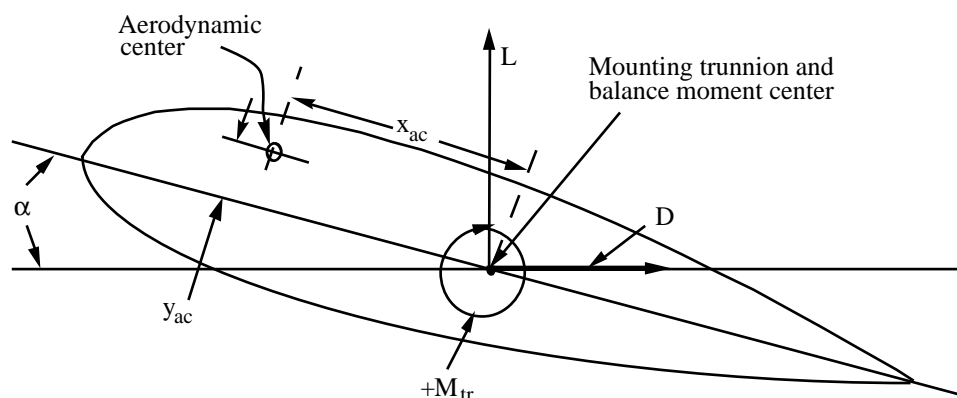


**Figure 4-4.** Wing showing position of aerodynamic center and mounting trunnion.

where  $c_t$  = wing tip chord and  $c_r$  = wing root chord for straight tapered wings, or

$$\text{MAC} = \frac{2}{S} \int_0^{b/2} c^2 dy$$

for other planforms.

Referring to Fig. 4-4 the pitching moment about the aerodynamic center is

$$M_{ac} = M_{tr} - x_{ac}(L \cos \alpha + D \sin \alpha) - y_{ac}(D \cos \alpha - L \sin \alpha) \quad (6)$$

where  $M_{tr}$  = the moment measured about the mounting trunnion. Hence, in coefficient form

$$C_{mac} = C_{mtr} - \frac{x_{ac}}{c} (C_L \cos \alpha + C_D \sin \alpha) - \frac{y_{ac}}{c} (C_D \cos \alpha - C_L \sin \alpha) \quad (7)$$

Because the pitching moment about the aerodynamic center,  $C_{mac}$ , does not vary with  $C_L$ , we have

$$\begin{aligned} \frac{dC_{mac}}{dC_L} = 0 &= \frac{dC_{mtr}}{dC_L} \\ &- \left[ \left( 1 + C_D \frac{d\alpha}{dC_L} \right) \cos \alpha + \left( \frac{dC_D}{dC_L} - C_L \frac{d\alpha}{dC_L} \right) \sin \alpha \right] \frac{x_{ac}}{c} \\ &- \left[ \left( \frac{dC_D}{dC_L} - C_L \frac{d\alpha}{dC_L} \right) \cos \alpha - \left( 1 + C_D \frac{d\alpha}{dC_L} \right) \sin \alpha \right] \frac{y_{ac}}{c} \end{aligned} \quad (8)$$

The experimental data is conveniently used to find  $C_L$ ,  $C_D$ ,  $\alpha$ , and also the slopes  $dC_{mtr}/dC_L$  and  $d\alpha/dC_L$ .

The determination of  $dC_D/dC_L$  is difficult because it is a curve. If the wing efficiency factor is available,  $dC_D/dC_L$  is found directly from

$$C_D = C_{D_{0_{\min}}} + \frac{C_L^2}{\pi \text{AR} e} \quad (9)$$

If not, the slope of the drag curve at the proper point is obtained using the mirror method. In this method, a small hand mirror is set directly on the plotted curve and adjusted until the reflected curve appears as a smooth continuation of the original. Under these conditions, the plane of the mirror is perpendicular to the drag curve at the selected  $C_L$ , hence, the drag curve slope is perpendicular to the mirror.

Substituting two points into Eq. (8), and solving the resulting pair of equations for  $x_{ac}$  and  $y_{ac}$  yields the required values. The approximate measurement of  $dC_D/dC_L$  is eliminated by selecting the angle at which  $C_D$  is a minimum for one of these points. At this point,  $dC_D/dC_L = 0$ .

To simplify locating the aerodynamic center, assume that the moment is due entirely to the lift and that the aerodynamic center is on the chord line (this is precisely true for a symmetrical airfoil); see Fig. 4-5.

Because the lift and drag act through the aerodynamic center, the moment about the trunnion is

$$M_{tr} = M_{ac} + L(h_{tr} - h_{ac})c \quad (10)$$

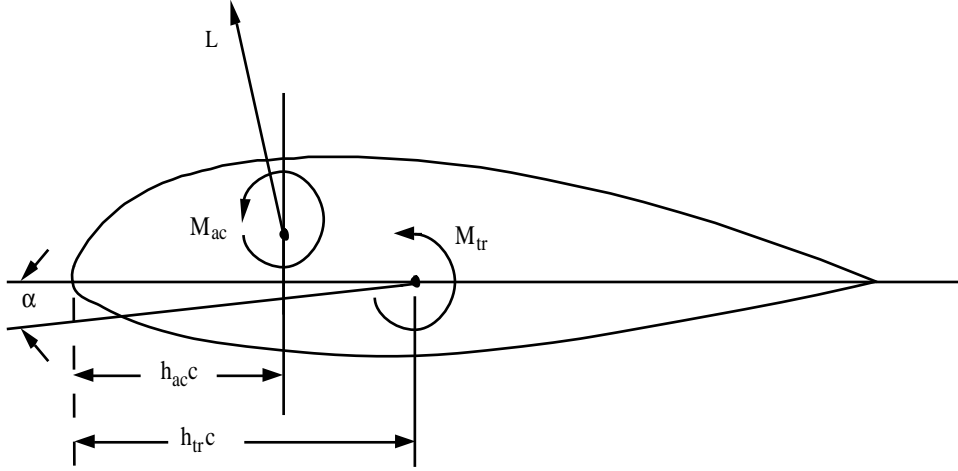


**Figure 4–5.** Pitching moments about the aerodynamic center and mounting trunnion.

where  $M_{ac}$  = moment about the aerodynamic center,  $h = x/c$  and  $h_{tr}$  = chordwise location of the balance trunnion.

Rewriting Eq. (10) in coefficient form, we have

$$C_{m_{tr}} = C_{m_{ac}} + C_L(h_{tr} - h_{ac}) \quad (11)$$

and after differentiating, transposing and noting that  $dC_{m_{ac}}/dC_L = 0$  we have

$$h_{ac} = h_{tr} - dC_{m_{tr}}/dC_L \quad (12)$$

The aerodynamic center is theoretically a small amount behind the quarter chord. In practice, it is found ahead of the quarter chord for the older profiles and behind for the new profiles.

Equation 11 indicates that when  $C_L = 0$ ,  $C_{m_{ac}} = C_{m_{tr}}$ . In other words, the value of the moment coefficient at the point where the curve strikes the  $C_L$ -axis is approximately the value of  $C_{m_{ac}}$ .

#### Pitching moment about the aerodynamic center: $C_{M_{ac}}$

After the location of the aerodynamic center is determined, the moment coefficient about it can be found from Eq. (7)

The value of  $C_{M_{ac}}$  varies with the amount and shape of the camber line. It is about zero for symmetrical wings and  $-0.007$  for an NACA 23012 airfoil section. It is not unusual to find some small spread in the values of  $C_{M_{ac}}$ , although the definition states that it must be constant.

## V. Balance Corrections

All balance readings must be corrected for the zero readings, i.e., the value of the scales under no-load conditions. These values are generally a function of angle-of-attack. The corrected scale readings then represent the aerodynamic forces and moments of

the model-support combination. That is

$$\begin{aligned} L_{\text{corr}} &= L_{\text{measure}} - L_0 \\ D_{\text{corr}} &= D_{\text{measure}} - D_0 \\ M_{\text{corr}} &= M_{\text{measure}} - M_0 \end{aligned} \tag{13}$$

The model supports not only affect the flow about the model but also have drag themselves. The effect on the flow about the model is called *interference* drag, the drag of the supports is called *tare* drag. The combination is called the *support* drag. Note that generally the aerodynamic effect on lift or moment is very small. Hence, corrections are not generally made.

The determination of the support drag is a complex task requiring imagination and considerable time for completion. The student's first reaction is to remove the model, measure the drag on the supports and call this support drag. This procedure fails to record either the effect of the model on the supports or the effect of the supports on the model.

One method of determining the support drag is as follows (see Pope, *Low Speed Wind Tunnel Testing* for others):

1. The model is tested in the normal manner; the data include both the model ( $D_N$ ) and the support drag ( $D_S$ ), i.e.

$$D_{\text{measure}} = D_{N_N} + D_{S_N} \tag{14}$$

2. Next, the model is inverted and the drag is measured, i.e.

$$D_{\text{measure}} = D_{N_I} + D_{S_I} \tag{15}$$

3. Then, with the model still inverted, dummy supports are installed in the tunnel ceiling. Instead of the clearance being between the dummy supports and the model, the normally exposed portion of the support strut (part marked A in Fig. 4-6) is attached to the model, and clearance is provided between the strut and the dummy support. This configuration yields

$$D_{\text{measure}} = D_{N_I} + D_{S_N} + D_{S_I} \tag{16}$$

The difference between Eqs. (16) and (17) yields  $D_{S_N}$ , which is then used in Eq. (14) to find the model drag.

## VI. Physical Set-up

The USNA 44 × 31 subsonic wind tunnel utilizes a pyramidal balance to support the model, to provide for changing its angle of attack and angle of yaw and to transmit the model loads into a system of linkages which separate them into their proper

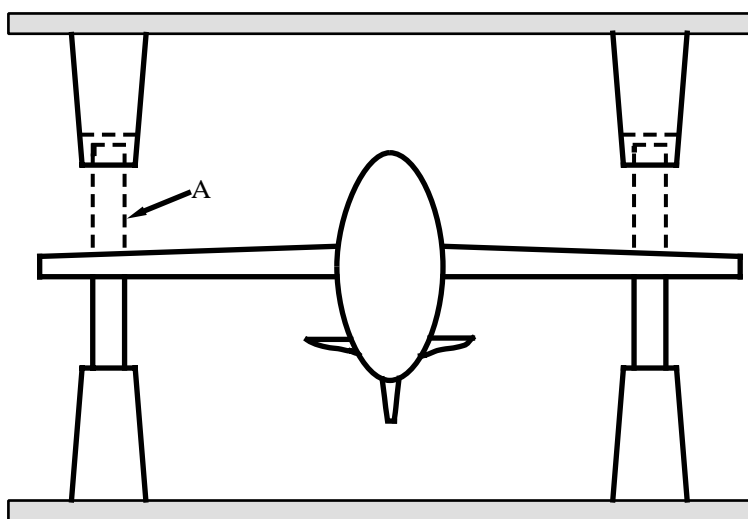


Figure 4-6. Method for determining support drag.

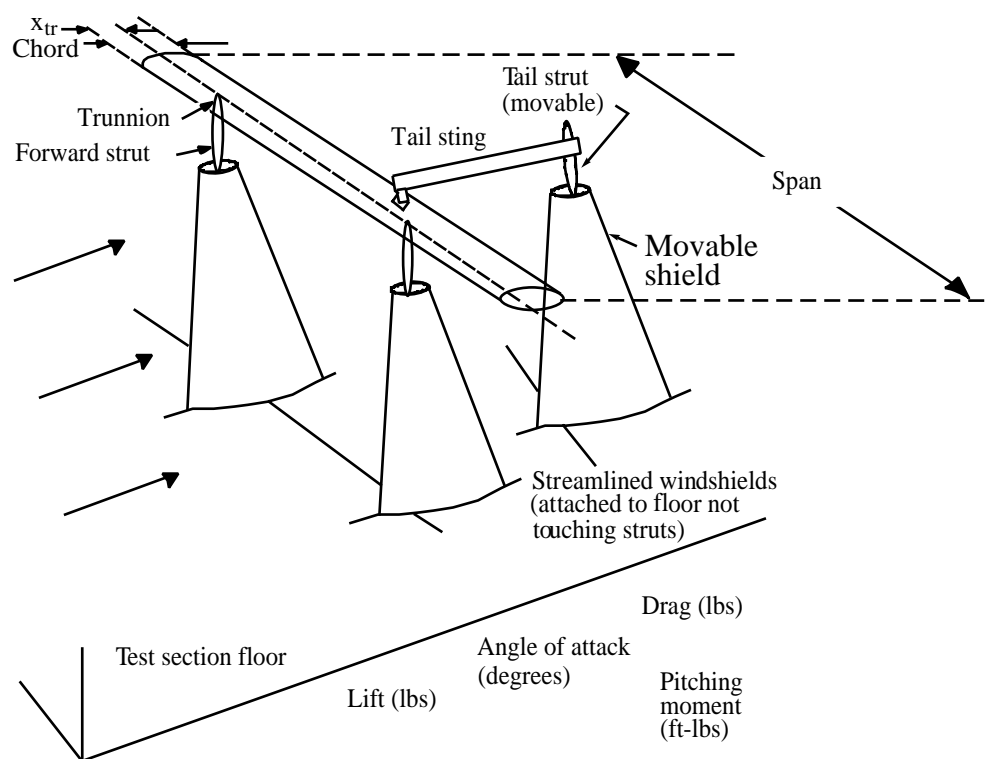


Figure 4-7. USNA triple support balance system.

components (see Fig. 4–7). A load cell system gives a direct reading of lift, drag and pitching moment in pounds and foot-pounds. These readings are affected by the drag of the exposed supports and by the interference of the struts on the free air flow about the model (and vice versa). Therefore, corrections are required to isolate the loads of the model alone.

Wings of varying aspect ratios are to be tested. The untwisted rectangular plan-form wings are of constant NACA 0012 section with a nine inch chord. The various aspect ratios are built up from several pieces as shown in Fig. 4–8.

The wings are floor mounted using a triple strut system that allows the wing to be rotated in pitch. The axis of rotation (or balance center) passes through the two forward support points (trunnions). The room thermometer, room barometer as well as the tunnel inclined manometer are utilized.

## VII. Procedure

1. Before starting the wind tunnel perform an auto zero.
2. Also before starting the wind tunnel obtain ‘tare’ values for lift, drag and pitching moment for angles of attack from  $-6^\circ$  to  $+18^\circ$  in  $2^\circ$  increments.
3. Determine the average lift, drag and moment tare values.
4. For each aspect ratio model measure the following:
  - a. wing span;
  - b. wing chord;
  - c. distance from the leading edge to the balance center.
5. Take data for each of the following aspect ratio models
  - a. short wing (A);
  - b. medium wing (B);
  - c. long wing (C);

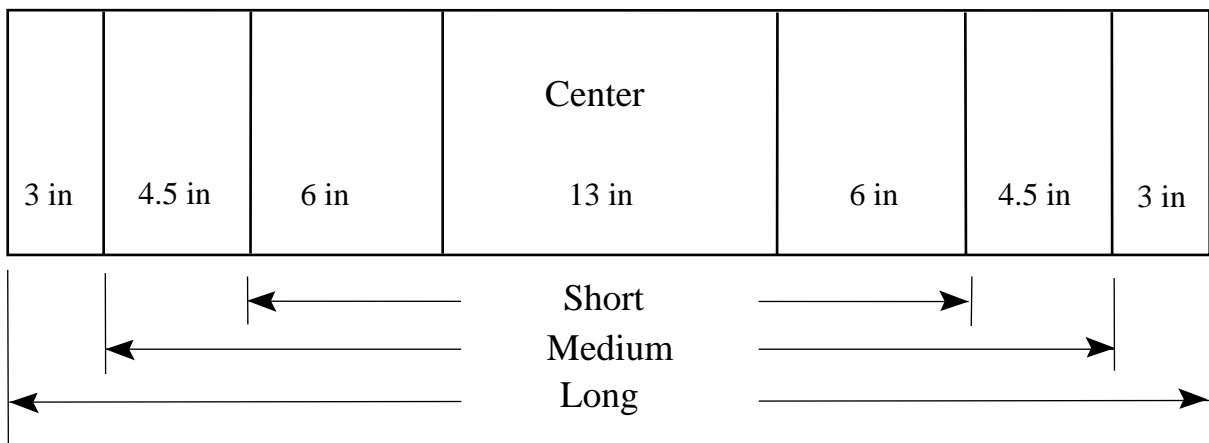


**Figure 4–8.** Aspect ratio model schematic.

6. For each configuration, take data for angles of attack settings from  $-6^\circ$  to  $+18^\circ$  (or until the model stalls) in  $2^\circ$  increments. Take extra data as required in the stall region, and at  $\alpha_{0L}$ . (Note: It will be necessary to shut down the tunnel for a short period in order to change configurations.)
7. For each configuration, make the usual measurements of barometric pressure, initial temperature and final temperature in order to calculate average freestream density and coefficient of viscosity.

## VII. Requirements

1. Calculate for the experiment:
  - a. average density;
  - b. dynamic pressure (utilizing the tunnel constant);
  - c. velocity;
  - d. effective Reynolds number.
2. Find or calculate for each angle of attack:
  - a. lift,  $L$ ;
  - b. drag,  $D$ ;
  - c. moment about the balance center,  $M_{BC}$ ;
  - d. lift coefficient,  $C_L$ ;
  - e. drag coefficient,  $C_D$ ;
  - f. moment coefficient about the balance center,  $C_{M_{BC}}$ ;
  - g. location of the aerodynamic center<sup>†</sup>;
  - h. wing efficiency factor,  $e$ ;
  - i. minimum drag coefficient.
3. Plot
  - a.  $C_L$  vs  $\alpha$
  - b.  $C_D$  vs  $\alpha$
  - a.  $C_{Mac}$  vs  $C_L$
4. Compare your experimental results with NACA section data.

## IX. Results

Fill in the following table.

Table 4-1.				
	NACA____			
Characteristic	section	$R_1 =$	$R_2 =$	$R_3 =$
theoretical $a$				
experimental $a$				
$C_{L\max}$				
$\alpha_{\text{Stall}}$				
$C_{D_{0\min}}^\dagger$				
$C_D$ at $C_{L\max}$				
$\alpha_{0L}$				
e				
$^\dagger$ * Correct for Re, if necessary				